Metamorphic GaAsP buffers for growth of wide-bandgap InGaP solar cells

J. Simon,[1,a)] S. Tomasulo,[1] P. J. Simmonds,[1] M. Romero,[2] and M. L. Lee[1]
[1]*Department of Electrical Engineering, Yale University, New Haven, Connecticut 06520, USA*
[2]*National Renewable Energy Laboratory, Golden, Colorado 80401, USA*

(Received 2 August 2010; accepted 10 November 2010; published online 5 January 2011)

$GaAs_xP_{1-x}$ graded buffers were grown via solid source molecular beam epitaxy (MBE) to enable the fabrication of wide-bandgap $In_yGa_{1-y}P$ solar cells. Tensile-strained $GaAs_xP_{1-x}$ buffers grown on GaAs using unoptimized conditions exhibited asymmetric strain relaxation along with formation of faceted trenches, 100–300 nm deep, running parallel to the $[0\bar{1}1]$ direction. We engineered a 6 μm thick grading structure to minimize the faceted trench density and achieve symmetric strain relaxation while maintaining a threading dislocation density of $\leq 10^6$ cm^{-2}. In comparison, compressively-strained graded $GaAs_xP_{1-x}$ buffers on GaP showed nearly-complete strain relaxation of the top layers and no evidence of trenches but possessed threading dislocation densities that were one order of magnitude higher. We subsequently grew and fabricated wide-bandgap $In_yGa_{1-y}P$ solar cells on our $GaAs_xP_{1-x}$ buffers. Transmission electron microscopy measurements gave no indication of CuPt ordering. We obtained open circuit voltage as high as 1.42 V for $In_{0.39}Ga_{0.61}P$ with a bandgap of 2.0 eV. Our results indicate MBE-grown $In_yGa_{1-y}P$ is a promising material for the top junction of a future multijunction solar cell. © *2011 American Institute of Physics*.
[doi:10.1063/1.3525599]

I. INTRODUCTION

Triple-junction metamorphic solar cells have reached efficiencies as high as 41.1% by combining lattice-mismatched, light-absorbing materials that target different regions of the solar spectrum[1]. Simulations indicate that efficiencies of 50%–60% may be attainable by increasing the number of junctions to 4–6, necessitating a wide-bandgap (E_g=2.0–2.2 eV) material to use as the top subcell.[2–5] Unfortunately, most III-V materials with the desired bandgap are indirect, demanding thick absorber layers in order to fully collect the incident sunlight. In addition, many of these materials contain Al, which has a strong propensity to form O-related deep levels,[6,7] resulting in solar cells with lower efficiencies.[8,9] In contrast, $In_yGa_{1-y}P$ (y=0.27–0.40) is an Al-free material with a direct bandgap in the desired range but is lattice-mismatched to conventional substrates such as GaAs and GaP. We therefore require a graded buffer to engineer the lattice constant and form a virtual substrate on which to grow wide-bandgap $In_yGa_{1-y}P$.

Previous work with graded $In_yGa_{1-y}P$ buffers on GaP resulted in phase separation that in turn led to higher than expected threading dislocation densities (TDDs).[10,11] In contrast, the mixed anion $GaAs_xP_{1-x}$ alloy covers the same range of lattice constants as the $In_yGa_{1-y}P$ system but does not phase separate.[12–14] We thus selected $GaAs_xP_{1-x}$ as the most suitable alloy system for our metamorphic virtual substrates. Mixed anion III-AsP buffers and light emitting devices based upon them have been investigated for several decades.[14–24] However, molecular beam epitaxy (MBE) growth of mixed anion III-AsP buffers for wide-bandgap photovoltaic devices has not been investigated.

In this work we studied the growth of metamorphic $GaAs_xP_{1-x}$ buffers, 2–6 μm thick, grown by solid-source MBE (SSMBE). We investigated both tensile (on GaAs) and compressive (on GaP) strained $GaAs_xP_{1-x}$ buffer systems, and examined the effect of growth conditions and buffer structure on material properties. We subsequently fabricated and tested wide-bandgap $In_yGa_{1-y}P$ solar cells grown on these graded buffers.

II. EXPERIMENTAL DETAILS

We grew all samples in a Veeco GEN-II SSMBE system on both GaAs (100) and GaP (100) on-axis substrates. Our system was equipped with elemental sources of Ga, In, Al, As, P, Si, and Be. The group V elements were thermally cracked to produce a dimer beam flux, and an ionization gauge was used to calibrate the beam equivalent pressures. Previous work has shown that $GaAs_xP_{1-x}$ composition is strongly dependent on growth temperature,[14–16] making it necessary to have a uniform substrate temperature across the wafer in order to achieve a homogeneous $GaAs_xP_{1-x}$ composition. We calibrated As composition (x) as a function of the beam equivalent pressures of both P_2 and As_2 at each growth temperature, and obtained an As composition uniformity of ±1% across a 4 inch wafer as estimated by photoluminescence (PL) measurements. We grew $GaAs_xP_{1-x}$ films at substrate temperatures (T_{SUB}) ranging from 580–700 °C in order to optimize growth conditions for both tensile and compressive buffers. For tensile-strained films the As_2/Ga flux ratio was kept constant at ~17, while the P_2 flux was varied in a step-wise fashion. For compressively-strained films we used P_2/Ga~8 and varied the As_2 flux at each step of the buffer. All buffers were capped with a 1 μm thick $GaAs_xP_{1-x}$ layer. The main variables used to optimize the relaxation, surface morphology, and TDD in the metamor-

a)Electronic mail: john.simonnavas@yale.edu.

phic buffers were the change in P composition in each step (ΔP), and the percentage lattice constant grading rate (ξ) given by:

$$\xi = \frac{a_s - a_c}{a_c d} \times 100\% \ \ \mu\text{m}^{-1}, \tag{1}$$

where a_s and a_c are the lattice constant of the substrate and $GaAs_xP_{1-x}$ capping layer, respectively, and d is the total thickness of the graded buffer.

After growth, we performed x-ray diffraction (XRD) measurements on a Bede D1 system with a Cu k_α source. X-ray scans satisfying the {004} and {224} Bragg conditions, with beams incident along both the [011] and [0$\bar{1}$1] in-plane directions, allowed us to extract the composition, tilt and relaxation of the samples. We used Nomarski optical microscopy, scanning electron microscopy (SEM), and atomic force microscopy (AFM) to characterize the surface morphology of our films. We prepared samples for plan-view and cross-sectional transmission electron microscopy (PVTEM and XTEM, respectively) by polishing them to a thickness of $\sim$10 μm, attaching them to a Cu aperture grid, and performing low angle Ar ion milling until they were electron transparent. Imaging was done in a Tecnai T12 system operated at 120 kV. XTEM enabled us to inspect defect and interface morphologies, while PVTEM allowed estimation of buffer TDD. We verified these TDDs using room temperature cathodoluminescence (CL) measurements performed on a JEOL-5800 SEM operated at 10 keV (penetration depth $\sim$1 μm) and an electron-beam current of 1 nA.

In the next part of the study, we grew $In_yGa_{1-y}P$ on $GaAs_xP_{1-x}$ buffers, by lowering T_{SUB} to 460 °C under the same As_2/P_2 overpressures used to grow the $GaAs_xP_{1-x}$ cap. We did not take any measures to prevent temperature-dependent surface anion exchange reactions that are known to be prevalent in metalorganic chemical vapor deposition (MOCVD) of $GaAs_xP_{1-x}$.[25] As_2 flux was closed for 1 min prior to the growth of $In_yGa_{1-y}P$ in order to minimize group V intermixing during growth. We performed room temperature PL on the films to determine their bandgaps with a 527 nm neodium doped Yttrium lithium flouride (Nd:YLF) laser.

Finally, we grew wide-bandgap $In_yGa_{1-y}P$ solar cells on graded p-$GaAs_xP_{1-x}$ on p-GaAs substrates. The device structure for all cells consisted of a 2 μm Be-doped $In_yGa_{1-y}P$ base with doping concentration of 10^{17} cm^{-3}, followed by a 100 nm Si-doped $In_yGa_{1-y}P$ emitter with a doping of 10^{18} cm^{-3} and a 20 nm window layer of Si-doped InAlP ($\sim 5\times10^{17}$ cm^{-3}), lattice matched to our junction. Finally, to facilitate Ohmic contact to the emitter we deposited a highly Si-doped ($\sim 5\times10^{18}$ cm^{-3}) GaAs layer in two stages. First we deposited $\sim$2 nm of n^+GaAs at 460 °C to protect the underlying InAlP window, and then we raised T_{SUB} to 580 °C to grow an additional 50 nm of n^+GaAs. We do not expect the lattice mismatch between the junction and the contact layer to adversely affect the efficiency of our device, since no minority carrier generation should take place near this interface. The type-II band offset between the low In-content InGaP and the InAlP window layer[26] dictates the $n-on-p$ polarity, since this configuration is expected to block valence band holes from traveling to the emitter contact but allow uninhibited flow of conduction band electrons.

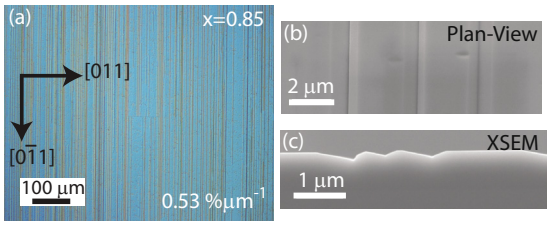

FIG. 1. (Color online) (a) Nomarski micrograph of $GaAs_xP_{1-x}$ films grown on GaAs with $\xi\sim0.53\%$ μm^{-1} and a top layer composition of x=0.85. Vertical lines are FTs formed during growth with $\rho_{FT}=120$ cm^{-1}. SEM images of trenches on $GaAs_xP_{1-x}$ layers (b) from plan-view and (c) cross-sectional view. A depth of 100–300 nm is measured for these FTs.

Following growth, we fabricated 2.1×2.1 mm^2 cells with 10% grid coverage. The top contact was a stack of 50 Å Ni followed by 1000 Å AuGe alloy (88–12 wt %), while the back p-type contact was 100 Å Cr followed by 1000 Å Au.

Finally, we measured the lighted I-V characteristics (L-IV) under approximate AM1.5G illumination using a Newport solar simulator with a Keithley 2400 source meter. External quantum efficiency (EQE) of the processed solar cells was measured in ac mode with a PV Measurements Inc. QEX7 system at 100 Hz.

III. RESULTS

A. Growth of metamorphic $GaAs_xP_{1-x}$ on GaAs

Initial $GaAs_xP_{1-x}$ buffers on GaAs consisted of a two-layer stack with a cap composition of x=0.85 grown at T_{SUB}=650 °C, and with $\xi\sim0.53\%$ μm^{-1}. Nomarski micrographs and planar view SEM images of these layers showed formation of faceted trenches (FTs) along the [0$\bar{1}$1] direction [Figs. 1(a) and 1(b)]. The FTs were 100–300 nm deep as measured by both cross-sectional SEM [Fig. 1(c)] and AFM. By measuring the angle between the facets and the growth plane we estimated their indices to be between (113)A and (114)A. The formation of FTs has been previously reported in other tensile-strained systems including InGaAs[27,28] and InGaP[29] on InP (100). XRD measurements showed asymmetric strain relaxation of these highly faceted films. France *et al.*[30] showed that the degree of relaxation along the orthogonal ⟨110⟩ directions in MBE-grown films is sensitive to growth conditions and that differences in α and β dislocation core structure are insufficient to account for the observed asymmetry. We thus explored different growth conditions to improve film relaxation and reduce FT formation.

In order to better understand the effect of growth conditions on the formation of FTs we determined their density (ρ_{FT}) by measuring the length of all facets and dividing by the sampled area. As we lowered ξ from 0.53 to $\sim$0.29% μm^{-1} with ΔP=4%, ρ_{FT} decreased by almost 30 times (from 119.7 to 4.3 cm^{-1}) for buffers with x>0.7. The strong dependence of ρ_{FT} on ξ suggests that the formation of FTs is affected by the kinetics of the strain relaxation process.

Increasing the growth temperature from 650 to 700 °C led to an increase in the relaxation of the top $GaAs_xP_{1-x}$ cap

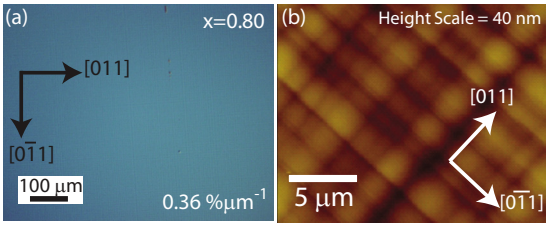

FIG. 2. (Color online) (a) Nomarski micrograph of a graded $GaAs_{0.80}P_{0.20}$ buffer grown on GaAs with $\xi \sim 0.36\%\ \mu m^{-1}$, $\rho_{FT}=0.73\ cm^{-1}$, and top layer composition of x=0.80. (b) AFM micrograph showing surface RMS roughness of 2.45 nm.

from ~60% to ~90%. Moreover, the strain relaxation was found to be almost completely symmetric, while ρ_{FT} decreased to 0.73 cm^{-1} [Fig. 2(a)]. AFM measurements revealed a surface root mean square (RMS) roughness as low as 2.45 nm across a $30\times30\ \mu m^2$ area on buffers graded to x=0.8 at $T_{SUB}=700\ ^\circ C$ [Fig. 2(b)]. PVTEM studies showed a reduction in the TDD from $2.0-3.0\times10^6\ cm^{-2}$ to $0.7-1.3\times10^6\ cm^{-2}$ [Fig. 3(a)] when T_{SUB} was increased from 650 to 700 °C on buffers with x>0.7. CL mapping of a $GaAs_{0.8}P_{0.2}$ graded buffer grown at 700 °C across an area of ~3200 μm^2 confirmed the low TDD of $10^6\ cm^{-2}$ obtained for the graded buffers grown at 700 °C [Fig. 3(b)]; these TDDs are comparable to those obtained in the highest efficiency metamorphic solar cells.[1,31]

Figure 4 shows TEM images taken of the FTs formed during growth of tensile strained $GaAs_xP_{1-x}$. We observed microtwins at the cusp of each FT, as well as evidence of dislocation pileups below the FTs. Microtwins[32,33] and surface roughness[34] have been shown in other material systems to block dislocation glide and, as a result, increase the TDD. Since FTs lead to higher TDD, they must be eliminated to realize large-area, high-efficiency solar cells.

When we attempted to increase the P content beyond 30% (x<0.7), ρ_{FT} increased to 120 cm^{-1}. Decreasing ξ to $0.19\%\ \mu m^{-1}$ with $\Delta P=4\%$ led to $\rho_{FT}\sim63\ cm^{-1}$ [Fig. 5(a)] but this ρ_{FT} is still almost 100 times higher than those obtained for buffers with x>0.7. XTEM also showed the formation of microcracks in tensile-strained buffers with x <0.7. By combining a low buffer grading rate with a reduced ΔP of 2% per step, we reduced ρ_{FT} to ~9 cm^{-1} [Fig. 5(b)]. Unfortunately, this requires the use of very thick buffers (~6–8 μm) in order to reach the desired lattice constants for growth of wide-bandgap $In_yGa_{1-y}P$. Graded buffers with $\rho_{FT}>60\ cm^{-1}$ exhibited an average TDD of

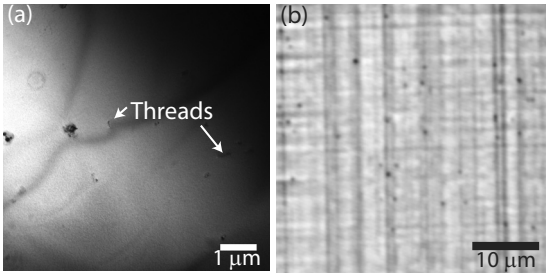

FIG. 3. Threading dislocations observed by (a) PVTEM (g=022) and (b) CL on tensile-strained $GaAs_xP_{1-x}$ buffers. Both PVTEM and CL comfirmed a TDD of $\sim10^6\ cm^{-2}$ for $T_{SUB}=700\ ^\circ C$.

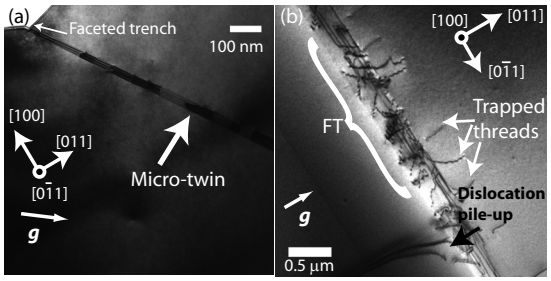

FIG. 4. (a) XTEM (g=−111) micrograph of a microtwin found below all FTs. (b) PVTEM (g=022) of FT showing dislocation pileups caused by FTs.

$\sim10^7-10^8\ cm^{-2}$ arising from the dislocation pile-ups associated with the FTs. Due to the inability to completely eliminate the FTs in tensile-strained $GaAs_xP_{1-x}$ with x<0.7, we also investigated the material properties of compressively-strained $GaAs_xP_{1-x}$ on GaP substrates.

B. Growth of metamorphic $GaAs_xP_{1-x}$ on GaP

Compressively-strained graded $GaAs_xP_{1-x}$ buffers, grown at a T_{SUB} of 580–620 °C and a V/III ratio of ~20, showed symmetric, and nearly complete strain relaxation of the buffer cap layer. These buffers had no FTs [Fig. 6(a)], microcracks, or dislocation pileups, evidence that FT formation is related to differences in strain relaxation mechanism for tensile and compressive (100) material. Due to the lack of FTs, we were able to use much higher strain grading rates than in the tensile-strained buffers, with ξ as high as $-1.23\%\ \mu m^{-1}$. AFM measurements across a $15\times15\ \mu m^2$ area gave an RMS surface roughness of ~3.56 nm on buffers graded to x~0.7 [Fig. 6(b)]. PVTEM measurements on buffers graded to x=0.68 revealed TDDs of $3\times10^6\ cm^{-2}$ when sampling an area of ~1000 μm^2 [Fig. 7(a)], while CL measurements gave a TDD of $1.5\times10^7\ cm^{-2}$ [Fig. 7(b)]. We speculate that variations in the measured TDDs arise from inhomogeneity across the sample. Our measured TDDs are ≥20 times higher than those reported for $GaAs_xP_{1-x}$ on GaP grown by MOCVD.[14] Factors leading to higher TDDs in MBE-grown graded $GaAs_xP_{1-x}$/GaP buffers remain unclear and will be investigated in future work.

C. Growth of metamorphic $In_yGa_{1-y}P$ on $GaAs_xP_{1-x}$

We subsequently grew layers of the wide-bandgap $In_yGa_{1-y}P$ absorber material onto both the tensile-strained and compressively-strained buffer systems. During the cool down of the $GaAs_xP_{1-x}$ buffer from 700 to 460 °C prior to growth of the $In_yGa_{1-y}P$, we observed a streaky reflection high energy electron diffraction (RHEED) pattern through-

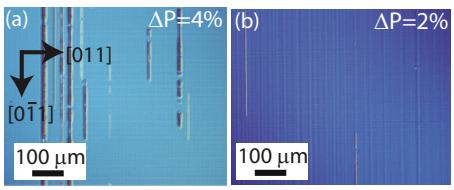

FIG. 5. (Color online) Nomarski micrographs of graded $GaAs_xP_{1-x}$ buffers with a top layer composition of x=0.68, $\xi\sim0.19\%\ \mu m^{-1}$, and ΔP of (a) 4% and (b) 2%. ρ_{FT} decreased from ~63 to 9 cm^{-1} by halving ΔP.

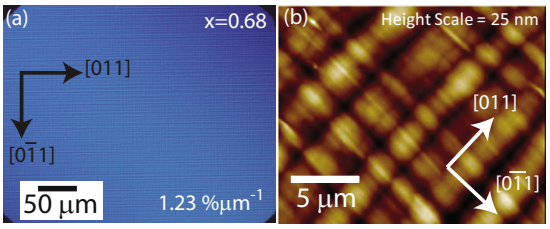

FIG. 6. (Color online) (a) Nomarski and (b) AFM micrographs of a compressively-strained $GaAs_xP_{1-x}$ buffer with a top layer composition of x=0.68 with $\xi \sim 1.23\%\ \mu m^{-1}$. A smooth morphology, with no FTs was observed, and a surface RMS roughness of ~3.56 nm was extracted from AFM.

out. This indicates that the surface morphology remained smooth during cool down, and implies that little surface anion exchange occurred.

By adjusting the lattice constant of the $GaAs_xP_{1-x}$ buffer cap, we were able to grow metamorphic $In_yGa_{1-y}P$ with bandgaps ranging from 1.88 to 2.16 eV. Our $In_yGa_{1-y}P$ films showed room temperature PL emission (Fig. 8) at bandgap energies that allow us to cover the range of values required for several proposed 4–6 junction cell designs.[2–4] Additionally, the bandgap of the lattice-matched $GaAs_xP_{1-x}$ beneath the $In_yGa_{1-y}P$ can reach values of ~1.9 eV, making it a suitable material for the second junction of a multijunction solar cell.[3,4]

AFM measurements on the $In_yGa_{1-y}P$ films showed similar surface morphologies to the underlying $GaAs_xP_{1-x}$ buffers, while XTEM studies of the $In_yGa_{1-y}P$ films revealed a smooth, coherent interface with the underlying $GaAs_xP_{1-x}$ cap (Fig. 9). The smooth interface confirms that minimal anion exchange occurred during cool down of the $GaAs_xP_{1-x}$ buffer surface prior to $In_yGa_{1-y}P$ growth. We performed selected area diffraction measurements along [011] and [0$\bar{1}$1] of the $In_yGa_{1-y}P$ films (Fig. 9 inset), and saw no evidence of the half-order superspots typical of CuPt ordering.[22] This indicates that our MBE-grown films are disordered, which agrees with previous results for MBE-grown $In_yGa_{1-y}P$.[35] CuPt ordering is often observed in MOCVD-grown $In_yGa_{1-y}P$ films, and small fluxes of Sb are typically used to promote disordered growth and to avoid ordering-induced bandgap reduction.[22] Sb is known to generate deep level defects in GaAs[36,37] and GaAsN[37–39] and can lead to elevated dark currents in InGaAsN solar cells.[38] Lower conductivity[40] and minority carrier lifetime[41] in InGaP solar cells have also been attributed to Sb incorporation. MBE-grown $In_yGa_{1-y}P$ does not appear to need an Sb surfactant to suppress CuPt ordering,[35] which may prove helpful in attaining wide-bandgap materials with long minority carrier lifetimes.

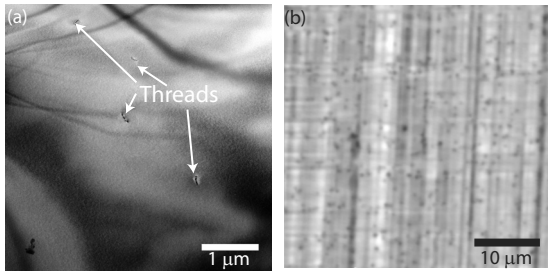

FIG. 7. (a) PVTEM (g=022), and (b) CL micrographs of compressively-strained $GaAs_{0.68}P_{0.32}$ buffers. The PVTEM survey showed TDD ~ 3×10^6 cm^{-2} while the CL showed TDD ~ 1.5×10^7 cm^{-2}.

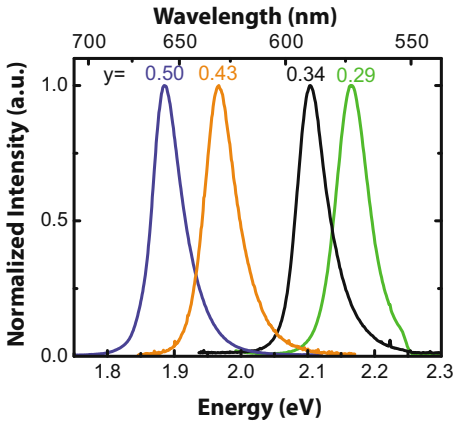

FIG. 8. (Color online) Normalized room temperature PL of metamorphic $In_yGa_{1-y}P$ films grown on $GaAs_xP_{1-x}$ with different In compositions.

D. $In_yGa_{1-y}P$ solar cells on metamorphic $GaAs_xP_{1-x}$

We grew solar cells using wide-bandgap $In_yGa_{1-y}P$ on graded $GaAs_xP_{1-x}$/GaAs, in order to investigate the photovoltaic properties of our material. A schematic of the finished devices is shown in the inset to Fig. 10(a). In addition to metamorphic cells with y=0.39 and 0.43, we grew a lattice-matched cell at y=0.48 as a control device (Table I). Bandgaps determined by PL ranged from 1.89–2.00 eV. The optimized grading procedure described in Sec. III A led to sufficiently low ρ_{FT} (<1 cm^{-1}) allowing us to process 2.1×2.1 mm^2 devices with no FTs. Under approximate AM1.5G illumination, we observed an increase in open circuit voltage (V_{oc}), and a decrease in short circuit current density (J_{sc}) in our $In_yGa_{1-y}P$ with decreasing y [Fig. 10(a)], consistent with expected trends for larger E_g.[42] Raising E_g from 1.89 to 2.00 eV resulted in an increase in V_{oc} from 1.31 to 1.42 V, while fill factors (FFs), and EQE_{max} [Fig. 10(b)] remained constant at ~0.8 and ~59%, respectively, for all

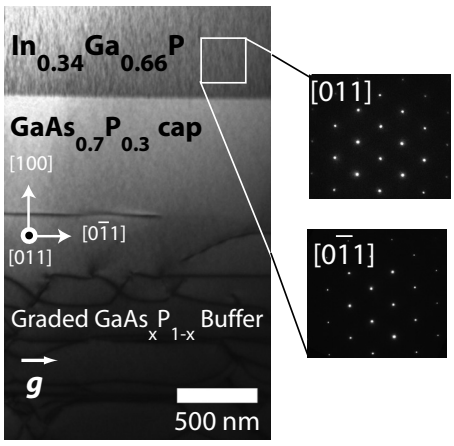

FIG. 9. XTEM (g=0$\bar{2}$2) of a lattice-matched $In_{0.34}Ga_{0.66}P$ layer on top of $GaAs_{0.7}P_{0.3}$ on GaAs. Threading dislocations are not formed at the $In_{0.34}Ga_{0.66}P/GaAs_{0.7}P_{0.3}$ interface. Insets at right show selected area diffraction patterns of the $In_{0.34}Ga_{0.66}P$ layer along both [011] and [0$\bar{1}$1] and show no evidence of CuPt ordering.

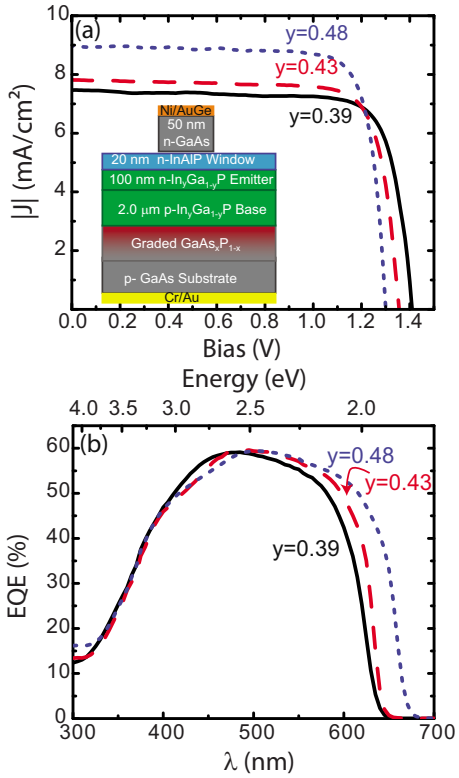

FIG. 10. (Color online) (a) L-IV characteristics under approximate AM1.5G illumination and (b) EQE measurements of $In_yGa_{1-y}P$ solar cells with 39% (—), 43% (– –), and 48% (- - -) In content. V_{oc} trends up with decreasing In content. Inset of (a) depicts solar cell growth structure.

devices (Table I). Note that the increase in V_{oc} of 0.11 V is proportional to the increase in E_g. Given the bandgap of 2.00 eV, our $In_{0.39}Ga_{0.61}P$ cell could be expected to generate a maximum V_{oc} of ~1.6 V ($V_{oc,max}=E_g/q-0.4$ V).[42] However, we believe that the V_{oc}, EQE, and FF of our metamorphic $In_yGa_{1-y}P$ cells are already quite promising in light of unoptimized processing and cell design. Refinements such as the addition of a back surface field and antireflection coatings should result in superior device performance in the future.

IV. CONCLUSIONS

We demonstrated the growth of metamorphic $GaAs_xP_{1-x}$ buffers under both tensile-strain (on GaAs) and compressive strain (on GaP) by SSMBE. Tensile-strained graded $GaAs_xP_{1-x}$ buffers suffered from high FT densities, which we were able to decrease by slowing the grading rate and reducing the compositional step size in the graded buffer. This allowed us to achieve a TDD of ~0.7–1.3 $\times 10^6$ cm^{-2} for a $GaAs_xP_{1-x}$ buffer with x=0.7. In comparison, compressively-strained $GaAs_xP_{1-x}$ graded buffers on GaP did not develop FTs but exhibited higher TDD. Metamorphic $In_yGa_{1-y}P$ grown on relaxed $GaAs_xP_{1-x}$ buffers showed no evidence of CuPt ordering, unlike similar films grown by MOCVD. We fabricated $In_{0.39}Ga_{0.61}P$ solar cells with a bandgap of 2.00 eV and a V_{oc} of 1.42 V.

TABLE I. Summary of solar cell device characteristics.

Composition	E_g (eV)	V_{oc} (V)	FF	EQE_{max} (%)	$\lambda_{EQE\ max}$ (nm)
$In_{0.48}Ga_{0.52}P$	1.89	1.31	0.80	59.4	505
$In_{0.43}Ga_{0.57}P$	1.97	1.37	0.79	59.7	495
$In_{0.39}Ga_{0.61}P$	2.00	1.42	0.80	59.1	485

The ability to increase both bandgap and V_{oc} by decreasing In content implies that further optimization could enable realization of efficient wide-bandgap cells for future 4–6 junction devices. In addition, it is straightforward to modify the design we presented here to accommodate growth of $In_yGa_{1-y}P$ with bandgaps in the range 1.9–2.2 eV. In the future, the wide-bandgap cell presented here could be incorporated into a multijunction spectrum splitting system,[5,43] or into an inverted metamorphic multijunction solar cell,[31] where the wide-bandgap cell is grown first followed by the subsequent junctions, allowing the substrate and $GaAs_xP_{1-x}$ graded buffer to ultimately be removed.

ACKNOWLEDGMENTS

We gratefully acknowledge Jung Han for access to characterization equipment, as well as funding from the Reid and Anne Buckley Foundation for Energy and the Environment and the NSF CAREER Program (Grant No. DMR-0955916).

[1]W. Guter, J. Schone, S. P. Philipps, M. Steiner, G. Siefer, A. Wekkeli, E. Welser, E. Oliva, A. W. Bett, and F. Dimroth, Appl. Phys. Lett. **94**, 223504 (2009).
[2]D. J. Aiken, A. B. Cornfeld, M. A. Stan, and P. R. Sharps, Proceedings of IEEE 4th World Conference on Photovoltaic Energy Conversion, Waikola, Hawaii, May 2006, Vol. 1,(IEEE, New York, 2006), pp. 838–841.
[3]I. Tobías and A. Luque, Prog. Photovoltaics **10**, 323 (2002).
[4]D. C. Law, R. R. King, H. Yoon, M. J. Archer, A. Boca, C. M. Fetzer, S. Mesropian, T. Isshiki, M. Haddad, K. M. Edmondson, D. Bhusari, J. Yen, R. A. Sherif, H. A. Atwater, and N. H. Karam, Sol. Energy Mater. Sol. Cells **94**, 1314 (2010).
[5]B. Mitchell, G. Peharz, G. Siefer, M. Peters, T. Gandy, J. C. Goldschmidt, J. Benick, S. W. Glunz, A. W. Bett, and F. Dimroth, "Four-junction spectral splitting photovoltaic receiver with high optical efficiency," Prog. Photovoltaics (to be published).
[6]C. T. Foxon, J. B. Clegg, K. Woodbridge, D. Hilton, P. Dawson, and P. Blood, J. Vac. Sci. Technol. B **3**, 703 (1985).
[7]T. Achtnich, G. Burri, and M. Ilegems, J. Vac. Sci. Technol. A **7**, 2537 (1989).
[8]C. Amano, K. Ando, and M. Yamaguchi, J. Appl. Phys. **63**, 2853 (1988).
[9]Y. Yazawa, T. Kitatani, J. Minemura, K. Tamura, K. Mochizuki, and T. Warabisako, Sol. Energy Mater. Sol. Cells **35**, 39 (1994).
[10]A. Y. Kim, W. S. McCullough, and E. A. Fitzgerald, J. Vac. Sci. Technol. B **17**, 1485 (1999).
[11]D. Gregušová, M. Kučera, S. Hasenöhrl, I. Vávra, P. Štrichovanec, J. Martaus, and J. Novák, Phys. Status Solidi C **4**, 1419 (2007).
[12]A. Zunger and S. Mahajan, *Materials, Properties and Preparation (Handbook on Semiconductors)* (North Holland, New York, 1994), Chap. 19.
[13]G. B. Stringfellow, J. Cryst. Growth **27**, 21 (1974).
[14]M. J. Mori, S. T. Boles, and E. A. Fitzgerald, J. Vac. Sci. Technol. A **28**, 182 (2010).
[15]B. W. Liang and C. W. Tu, J. Appl. Phys. **74**, 255 (1993).
[16]A. Yu. Egorov, A. R. Kovsh, V. M. Ustinov, A. E. Zhukov, P. S. Kop'ev, and C. W. Tu, J. Cryst. Growth **188**, 69 (1998).
[17]C. T. Foxon, B. A. Joyce, and M. T. Norris, J. Cryst. Growth **49**, 132 (1980).
[18]D. Wildt, J. Vac. Sci. Technol. B **16**, 1804 (1998).
[19]M. S. Abrahams, J. Appl. Phys. **40**, 3754 (1969).
[20]T. Tanaka, K. Uchida, Y. Ishitani, and S. Minagawa, Appl. Phys. Lett. **66**, 783 (1995).
[21]J.-F. Lin, M.-C. Wu, M.-J. Jou, C.-M. Chang, and B.-J. Lee, J. Cryst. Growth **137**, 400 (1994).

[22]M. A. Steiner, L. Bhusal, J. F. Geisz, A. G. Norman, M. J. Romero, W. J. Olavarria, Y. Zhang, and A. Mascarenhas, J. Appl. Phys. **106**, 063525 (2009).
[23]M. K. Hudait, J. Appl. Phys. **95**, 3952 (2004).
[24]W. Zhang, C. Yi, and A. Brown, J. Vac. Sci. Technol. B **25**, 960 (2007).
[25]M. J. Mori and E. A. Fitzgerald, J. Appl. Phys. **105**, 013107 (2009).
[26]I. Vurgaftman, J. R. Meyer, and L. R. Ram-Mohan, J. Appl. Phys. **89**, 5815 (2001).
[27]G. Wagner and P. Paufler, Phys. Status Solidi A **138**, 389 (1993).
[28]A. Ponchet, A. Le Corre, A. Godefroy, S. Salaün, and A. Poudoulec, J. Cryst. Growth **153**, 71 (1995).
[29]F. Cléton, B. Sieber, A. Lefebvre, A. Bensaada, R. A. Masut, J. M. Bonard, J. D. Ganière, and M. Ambri, J. Appl. Phys. **80**, 827 (1996).
[30]R. France, A. J. Ptak, C.-S. Jiang, and S. P. Ahrenkiel, J. Appl. Phys. **107**, 103530 (2010).
[31]J. F. Geisz, D. J. Friedman, J. S. Ward, A. Duda, W. J. Olavarria, T. E. Moriarty, J. T. Kiehl, M. J. Romero, A. G. Norman, and K. M. Jones, Appl. Phys. Lett. **93**, 123505 (2008).
[32]L. Lu, Y. Shen, X. Chen, L. Qian, and K. Lu, Science **304**, 422 (2004).
[33]M. L. Lee, D. A. Antoniadis, and E. A. Fitzgerald, Thin Solid Films **508**, 136 (2006).
[34]S. B. Samavedam and E. A. Fitzgerald, J. Appl. Phys. **81**, 3108 (1997).
[35]J. Sang, J. W. Steeds, and M. Hopkinson, Semicond. Sci. Technol. **8**, 502 (1993).
[36]R. Yakimova, P. Omling, B. H. Yang, L. Samuelson, J.-O. Fornell, and L. Ledebo, Appl. Phys. Lett. **59**, 1323 (1991).
[37]W. K. Cheah, W. J. Fan, S. F. Yoon, K. H. Tan, R. Liu, and A. T. S. Wee, Thin Solid Films **488**, 56 (2005).
[38]A. J. Ptak, D. J. Friedman, and Sarah Kurtz, J. Vac. Sci. Technol. B **25**, 955 (2007).
[39]W. K. Cheah, W. J. Fan, S. Wicaksono, S. F. Yoon, and K. H. Tan, J. Cryst. Growth **254**, 305 (2003).
[40]J. M. Olson, W. E. McMahon, and S. Kurtz, Proceedings of IEEE Fourth World Conference on Photovoltaic Energy Conversion, Waikola, Hawaii, May 2006, Vol. 1, (IEEE, New York, 2006), pp. 787–790.
[41]C. M. Fetzer, R. T. Lee, G. B. Stringfellow, X. Q. Liu, A. Sasaki, and N. Ohno, J. Appl. Phys. **91**, 199 (2002).
[42]R. R. King, D. C. Law, K. M. Edmondson, C. M. Fetzer, G. S. Kinsey, H. Yoon, R. A. Sherif, and N. H. Karam, Appl. Phys. Lett. **90**, 183516 (2007).
[43]A. Barnett, D. Kirkpatrick, H. Christianan, M. Duncan, W. Mark, E. Keith, S. Richard, C. Dave, B. Stuart, A. Dan, G. Allen, K. Sarah, K. Larry, S. Myles, G. Jeffery, D. Tom, B. Roger, T. Laszlo, S. Narkis, B. John, J. Omkar, G. Keith, K. Fouad, D. Alan, F. Ian, U. Blair, S. Greg, C. Eric, and S. David, Prog. Photovoltaics **17**, 75 (2009).